**Preprints of the 19th World Congress**
**The International Federation of Automatic Control**
**Cape Town, South Africa. August 24-29, 2014**

# Robust Position Tracking Control and Ground Contact Detection of a Cheetaroid-I Leg by a Disturbance Observer

**Jungsu Choi, Byeonghun Na, Sehoon Oh, and Kyoungchul Kong** *

* *Department of Mechanical Engineering, Sogang University, Seoul, Korea (Tel: +82-2-705-4766; e-mail: kckong@sogang.ac.kr).*

**Abstract:** Quadruped robot systems are being intensively investigated as a new means of transportation systems with multi-purposes. As the operation conditions of such systems, such as a payload and gait speed, are demanding, the control of the robotic legs is challenging. In addition, the dynamics of such systems is subjected to large disturbances and parameter variations due to the ground contact and the complicated mechanical structure. In this paper, a robust control algorithm based on a disturbance observer (DOB) is proposed for the control of legs of a quadruped robot, Cheetaroid-I. The DOB enables rejecting disturbances caused by the ground contact, payload, etc, and detecting the ground contact without force sensors. The proposed method is verified by experimental results.

## 1. INTRODUCTION

Importance of robotic systems has risen in the modern society. Their applications have been extended to not only industrial automation, but also the daily life of humans (K. Kong *et al.* [2012]). Various robots have been developed for helping humans in recent years. With a great amount of government support, many researchers are making their best efforts to develop robot systems that can replace the role of humans in hazardous and dangerous environments, in particular the disastrous areas by a nuclear accident (J. Savall *et al.* [1999], K. Nagatani *et al.* [2011], and K. Kaneko. [2012]). Considering the required dexterousness and agility of robot systems, legged locomotion systems are being intensively investigated. In particular, quadruped robots are receiving great attention as a new means of transportation for various purposes, such as military, welfare, and rehabilitation systems. The use of four legs enables a robustly stable gait; compared to the humanoid robots, the quadruped robots are particularly advantageous in improving the locomotion speed, the maximum payload, and the robustness toward disturbances, e.g., refer to M. Raibert *et al.* [2008], M. A. Lewis *et al.* [2011], and B. Na *et al.* [2013].

The more demanding conditions robots are exposed to, however, the more challenging the control of robotic legs becomes. As the gait speed increases, the frequency bandwidth of reference signals (i.e., desired motions) is also significantly enlarged. Thus the significant enlargement of closed-loop bandwidth of a control system is necessary. Consequently, high gain control with a high-speed data acquisition system is unavoidable, which also necessitates the accurate measurement of physical states without noise. Moreover, the dynamics of a robotic leg is highly uncertain and time-varying due to the ground contact and the ground condition, as well as the unknown payload. Therefore, a control algorithm that can achieve both great control performance and stability robustness is essential for the effective control of a quadruped robot.

In this paper, a robust control algorithm is proposed for a high-speed quadruped robot, Cheetaroid-I. The Cheetaroid-I is a bio-inspired robot system, the skeletal structure of which is inspired from animals that run fast. The leg system of Cheetaroid-I, which consists of three active joints, is particularly designed for improved gait-stability during a high-speed locomotion. The control of the Cheetaroid-I leg, however, is challenging because of the large weight of the robot body, the model change due to the ground contact, the high-frequency reference trajectory, and so on. In order to achieve great control performance rejecting the disturbances from the ground and the model change, a disturbance observer (DOB) is utilized in the control of a Cheetaroid-I leg system in this paper.

The DOB estimates external disturbances by comparing an actual measurement with a simulated output. By filtering the output discrepancy with an inverse of the system model, the estimation of the exogenous disturbance is achieved (K. Ohnishi. [1987] and K. Fujiyama *et al.* [1998]). The DOB can also be applied as a feedback controller, in which case the disturbance is rejected and the overall system is controlled to follow the nominal model, as reported in the papers of (K. Kong *et al.* [2009], T. Umeno *et al.* [1991], and S. Oh *et al.* [2013]). Since it attenuates the model change and makes the closed-loop system robust toward the external disturbances, the DOB is appropriate for the Cheetaroid-I leg control. For the appropriate design of the DOB (i.e., appropriate selection of a nominal plant structure and its parameters), reliable knowledge on the nominal plant dynamics and the range

⋆ This work was supported by the National Research Foundation of Korea (NRF) grant funded by the Korea government (MSIP) (NRF-2012R1A1A1008271).

 

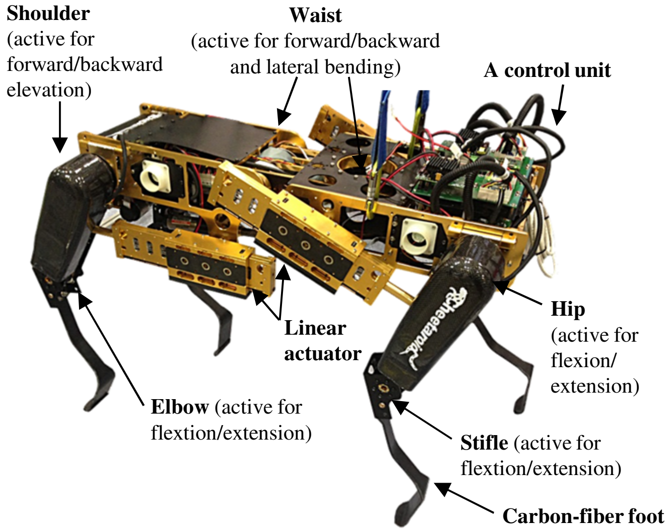


Fig. 1. Configuration of Cheetaroid-I.

of dynamics variation is required, which is challenging in practice.

In this paper, the dynamic model of a Cheetaroid-I leg system is analyzed, and the nominal plant model and the range of model variations are obtained through extensive experiments. The implementation of the DOB, however, requires extra care due to the unstable zero of the plant dynamics. Therefore, the parameters of the nominal plant model are further optimized considering the closed-loop stability of the DOB, as well as the closed-loop performance. The proposed model optimization process enables the effective control of the robotic leg without performance degradation even in the presence of an unstable zero in the nominal plant model, which is the case of Cheetaroid-I.

In addition to robust stabilization and disturbance rejection, the DOB is also utilized to detect the ground contact, which is necessary information for a higher level motion control algorithm. While the majority of the disturbances estimated by the DOB is due to the ground contact, observation of the ground contact is available by monitoring the magnitude of the estimated disturbance. Consequently, the proposed control system enables both effective control of a Cheetaroid-I leg system and removal of force sensors for detecting the ground contact.

## 2. CHEETAROID-I ROBOT SYSTEM

### *2.1 System Configuration*

Cheetaroid-I is a quadruped robot that has fourteen degrees of freedom (DoFs), which include three DoFs in each leg system and two DoFs at the waist, as shown in Fig. 1. It is capable of generating various locomotion types, such as different gait phases, gyrations, and so on. The hip and shoulder joints are equipped with customized linear actuators that exhibit high power output with low mechanical impedance. For the details on the design of Cheetaroid-I (B. Na *et al.* [2013]).

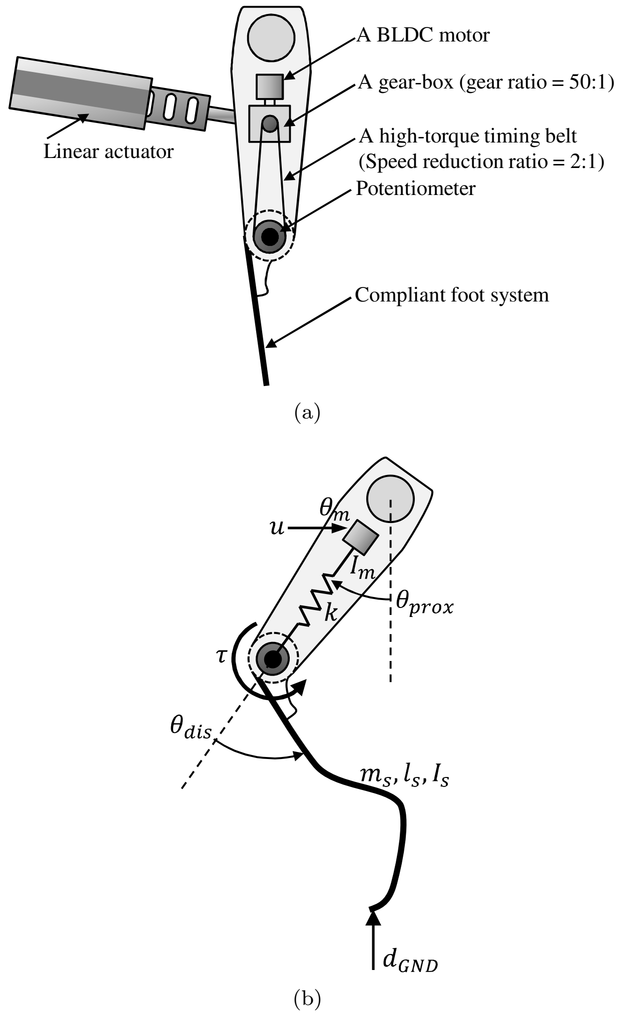


Fig. 2. The schematic of a leg system; (a): design of a hind leg, and (b): a simplified model for dynamics analysis.

### *2.2 Modeling of a Leg System*

Each of the Cheetaroid-I legs has three actuators; one for the flexion/extension of the hip/shoulder joint, one at the stifle/elbow joint, and one for the abduction/abuction movements. The upper leg is composed of thin aluminum frames with carbon-fiber-reinforced-plastic (CFRP) housings, so that it is rigid. On the other hand, the lower leg is made of compliant CFRP material for the absorption of impacts due to the ground contact. Figure 2(a) shows the design of a leg system. As shown in the figure, the proximal joint (i.e., the hip or the shoulder joint) is actuated by a powerful linear actuator. On the other hand, the distal joint (i.e., the stifle or the elbow joint) is actuated by a compact and light-weight brushless DC motor (50W, Maxon Motor Co.) for the sake of the minimal moment of inertia of the leg system. In addition, the motor is installed near the proximal joint, while the actuation torque is transferred via a timing belt. This design provides the great controllability of a distal joint (i.e., the angular position of the foot system) while reducing the moment of inertia of the upper leg part.

The compliance of the timing belt, however, creates a challenge in the control, since it is placed between the motor, where a control input takes place, and the joint, where the output is measured. The compliance increases the order of the plant model (i.e., the number of poles in the plant transfer functions) and also imposes zeros occasionally. Notice that the equations of motion of the motor and the foot system are respectively

$$I_m\ddot{\theta}_m + k(\theta_m - \theta_{dis}) = u \tag{1}$$

and

$$I_s(\ddot{\theta}_{dis}+\ddot{\theta}_{prox})+c_p\dot{\theta}_{dis}+m_sgl_s\sin(\theta_{dis}+\theta_{prox}) = \tau+d \tag{2}$$

where $\tau = k(\theta_m - \theta_{dis})$ is the torque transmitted by the timing belt, and $d = d_{GND}l_s\sin(\theta_{dis} + \theta_{prox}) + f(\ddot{\theta}_{prox}, \dot{\theta}_{prox})$ is the disturbances due to the ground contact and the motion of the upper leg part. Although the equations of motion in (1) and (2) are subjected to large disturbances and model discrepancies due to the inherent complexity of a robot system, transfer functions can be obtained rearranging and linearizing the equations above, i.e.

$$\theta_{dis}(s) = G_{u\to\theta_{dis}}u(s)+G_{\theta_{prox}\to\theta_{dis}}\theta_{prox}(s)+G_{d_G\to\theta_{dis}}d(s) \tag{3}$$

where $\theta_{dis}(s)$, $u(s)$, $\theta_{prox}(s)$, $d(s)$ are the Laplace transforms of $\theta_{dis}(t)$, $u(t)$, $\theta_{prox}(t)$, $d(t)$, respectively. Notice that the angular position of the distal joint, i.e., $\theta_{dis}$, is influenced by the motion of the upper part and the disturbances, as well as the control input, $u$. Assuming that the second and third terms on the right-hand-side of (3) are disturbances to be rejected, the structure of a nominal plant dynamics (i.e., $G_{u\to\theta_{dis}}$) can be obtained. Rearranging (1) and (2), one can easily find that $G_{u\to\theta_{dis}}$ is a fourth-order transfer function with no zero.

Among the three active DoFs in each leg of the Cheetaroid-I, the control method for distal joint (i.e., the elbow/stifle joint) is introduced in this paper.

### *2.3 System Identification of a Nominal Plant Dynamics*

In order to identify the parameters of $G_{u\to\theta_{dis}}$, system identification experiments were carried out. In the experiments, the control input, $u(t)$, was the pulse width in the range of $[-20000, 20000]$, and the output was the stifle/elbow joint angle in the unit of radians. Eight sets of experiments were conducted with different input magnitudes. Each set of experiments consisted of sinusoidal waves with different frequencies. Once a set of experimental data was obtained, both the input and output signals were Fourier-transformed, and frequency responses were obtained by comparing the input and output signals in the frequency domain.

Figure 3 shows the experimental results. It should be noted that the magnitudes and phases did not exactly match as the input magnitude changed. This implies that the system has nonlinearities or time-varying components. In particular, the model variation was significant at low and high frequencies, where the low frequency uncertainty was mainly due to the friction of the joint, and that of the high frequency was due to the inaccuracy of sensor measurement, noise, and so on. Consequently, a band is formed [see the circles in the figure] and the parameters of $G_{u\to\theta_{dis}}$ was obtained considering the magnitude and phase bands as

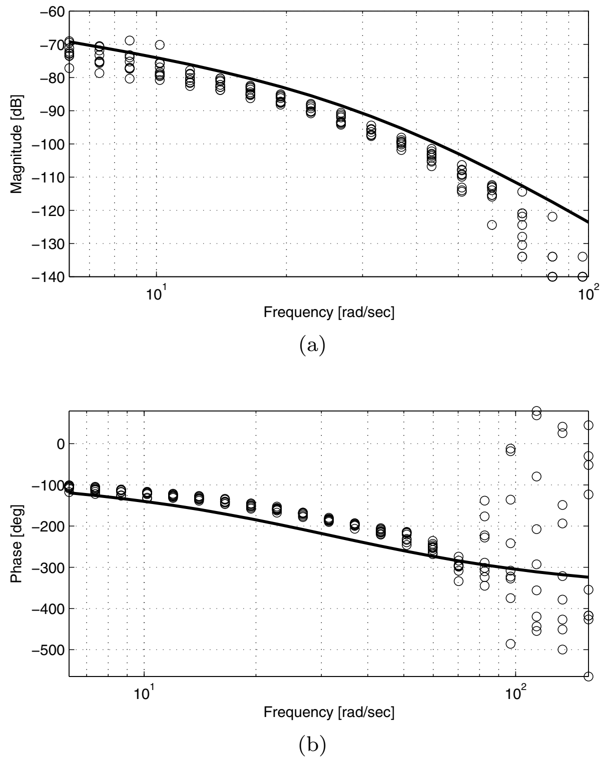


(a)

(b)

Fig. 3. System identification experiments and a nominal plant model; (a): magnitudes, and (b): phases.

$$G_{u\to\theta_{dis}} = \frac{78}{s^4 + 101s^3 + 3275s^2 + 35360s + 16880} \tag{4}$$

The frequency response of the obtained nominal plant model in (4) is also shown in Fig. 3 [see the continuous lines in the figure].

### *2.4 Identification of Dynamics Uncertainties*

Since both the nominal plant model and experimental data are available, multiplicative uncertainties can be obtained by

$$\mathbf{\Delta}(jw) = \frac{G_{exp}(jw) - G_{u\to\theta_{dis}}(jw)}{G_{u\to\theta_{dis}}(jw)} \tag{5}$$

The calculated $\mathbf{\Delta}(jw)$ for every experiment in Fig. 3 is shown in Fig. 4. It should be noted that the magnitudes of the model mismatch are large at high frequencies. For the simplicity of the uncertainty modeling, it is assumed that $\mathbf{\Delta} \in \{W\Delta; W \in \mathbb{S}, \|\Delta\|_\infty < 1\}$, where $W(s)$ is a minimum-phase transfer function that represents the upper bound of multiplicative uncertainties at each frequency. Then, the upper bound of the multiplicative uncertainties can be modeled based on the experimental fata shown in Fig. 4, i.e.,

$$W(s) = \frac{0.011s^2 + 1.011s + 22.933}{s + 30.000} \tag{6}$$

The magnitude of $W(jw)$ is also shown in Fig. 4 [see the continuous line].

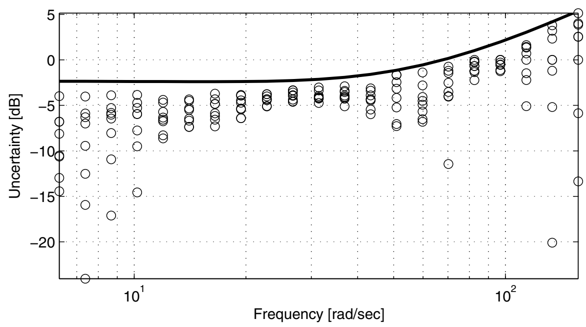


Fig. 4. The upper bound of the multiplicative uncertainties.

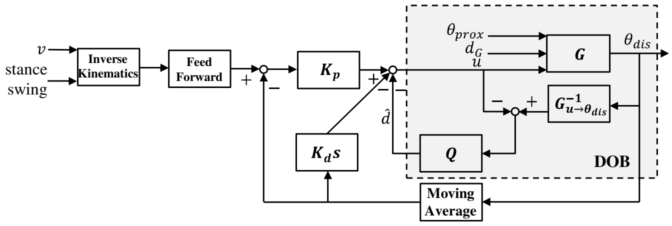


Fig. 5. The block diagram of the disturbance observer.

## 3. DISTURBANCE OBSERVER DESIGN FOR LEG CONTROL

### *3.1 Overall Controller Structure*

The overall control algorithm includes a feedforward filter, the feedback controller, and the DOB, as shown in Fig 5. Since the DOB is not a tracking controller, the feedback (PD) controller is applied as an outer loop of the DOB. If the plant has unstable poles, careful consideration should take place in the design of the controller. In the leg of the Cheetaroid-I, the plant dynamics does not possess any poles outside of the unit circle on the $z$-plane. On the other hand, the reference trajectory of the Cheetaroid-I is generated by inverse kinematics. Since the reference trajectory is generated by considering only the possibility of locomotion, the drastically changing moments exist in the reference trajectory. Therefore, the derivative controller calculates the control input by using only the output of the plant. Assuming that the DOB loop behaves as its nominal model, the feedforward controller is designed based on the closed-loop characteristics formed by the PD controller and the nominal model. A moving average filter is used to reduced the sensor noise.

### *3.2 Design of a Q-filter*

In the design of $Q$-filter, the following conditions should be fulfilled to guarantee robust stability:

(1) $Q$-filter must be stable, and
(2) the magnitude of $Q(jw)$ should be less than that of $W^{-1}(jw)$ for all $w \in \mathbb{R}_+$.

Based on the experimentally obtained $W(s)$ in (6), a $Q$-filter can be designed such that its magnitude is smaller than that of $W^{-1}(jw)$ at the entire frequency range. A possible $Q(s)$ is

$$Q(z) = \frac{0.218}{z^2 - 1.067s + 0.285} \qquad (7)$$

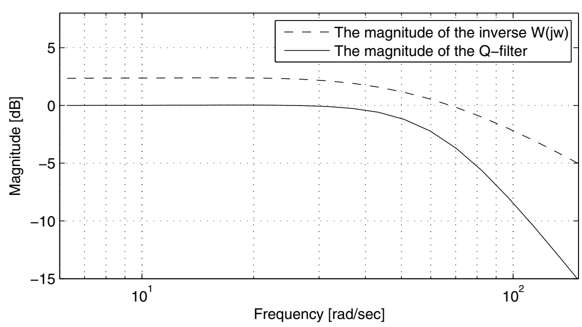


Fig. 6. The magnitudes of the inverse $W(jw)$ and the Q-filter.

Note that $Q(s)$ in (7) has the cutoff frequency of 10 Hz and the magnitude of 1 at low frequencies. Also, it has the robust stability margin of at least 3 dB for all frequencies, as shown in Fig. 6. For the implementation of $Q(s)$, an equivalent filter in the discrete time domain, i.e., $Q(z)$, can be obtained by the pole-zero matching method.

### *3.3 Disturbance Observer Stabilization*

The nominal plant model, $G_{u\to\theta_{dis}}(s)$, is discretized for implementation. The discretized nominal plant model is

$$G_{u\to\theta_{dis}}(z) = \frac{10^{-7}(0.267z^3 + 2.408z^2 + 1.969z + 0.146)}{z^4 - 3.152z^3 + 3.692z^2 - 1.906z + 0.366} \qquad (8)$$

Note that zeros of $G_{u\to\theta_{dis}}(z)$ placed at $-0.082$, $-0.818$, and $-8.134$, and an unstable zero is introduced during discretization. In the DOB loop, since the inversed nominal plant, $G^{-1}_{u\to\theta_{dis}}(z)$, is used for estimation of the disturbance, the unstable zero of $G_{u\to\theta_{dis}}(z)$ may introduce in stability into the DOB loop. Therefore, the unstable zero derived from discretization should be removed for the stability of the DOB. In this aspect, a modified nominal plant model, $G_{mod}(z)$, is

$$G_{mod}(z) = \frac{10^{-7}(2.434z^2 + 2.191z + 0.164)}{z^4 - 3.152z^3 + 3.692z^2 - 1.906z + 0.366} \qquad (9)$$

It is important that, the dynamic characteristics of the nominal model is not significantly changed for the effectiveness of the DOB, even if the nominal plant model is changed as from (8) to (9). Figure 7 shows the Bode plots of the nominal plant model and the modified nominal plant model. While unstable zero is removed in the modified plant model, the frequency characteristics of the system are not changed, as shown in the figure. Therefore, the modified nominal plant model is suitable for the implementation of the DOB.

## 4. EXPERIMENTAL RESULTS

### *4.1 Reference Tracking Performance Evaluation*

Figure 8 shows the experimental results of the PD controller without the DOB; the reference trajectory and the controlled joint angle are shown in the figure. The locomotion speed was increased gradually in the experiment. Recall that, since the reference trajectory has drastically changing moments, the derivative controller was designed such that it calculates the control input by using only

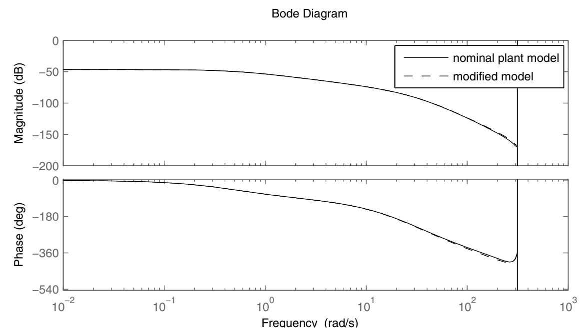


Fig. 7. Bode plot of the nominal plant model and modified model.

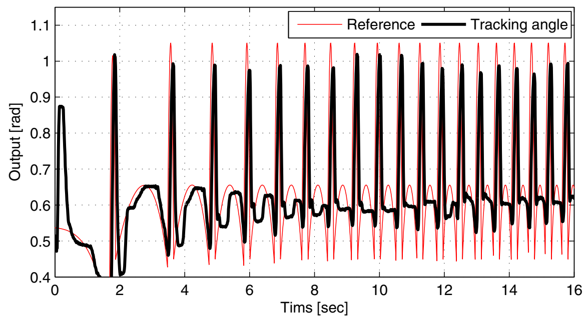


Fig. 8. Tracking performance with the PD control only.

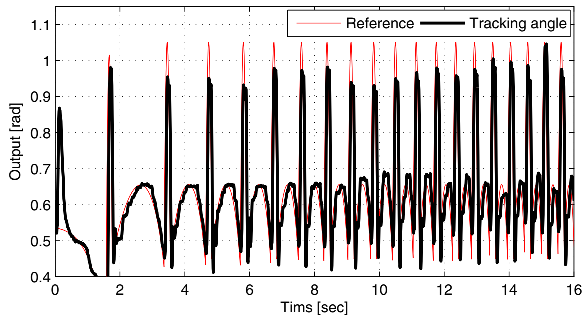


Fig. 9. Tracking performance with the proposed control method.

the output of the plant not including the reference signal. Nevertheless, the tracking performance of the PD controller was insufficient to realize successful locomotion. It was difficult to obtain the desired performance only with the PD control, because the gear-box and the timing belt increased the response time during force transmission. The backlash of the gear-box and the timing belt significantly affected the tracking performance. Moreover, the tracking performance was more deteriorated as the locomotion speed of the Cheetaroid-I increased. This is because the reduced stance period made the change of the reference trajectory more drastic.

The tracking performance with the proposed control method is shown in Fig. 9, where the performance was remarkably improved than the PD controller by the proposed control method. In both experiments in Figs. 8 and 9, the same gains were used in the PD controller. Since disturbances and model uncertainties by the gear-box and the timing belt were significantly rejected by the

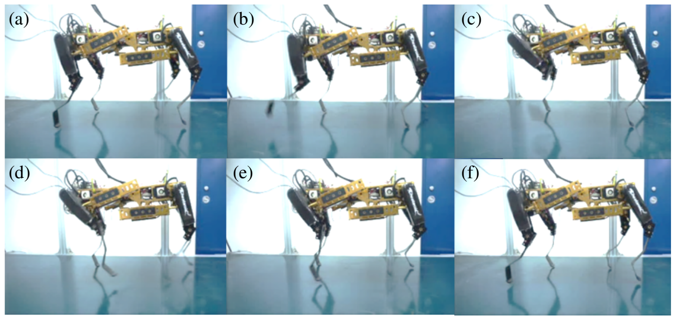


Fig. 10. Snapshots of a video of a gait control experiment.

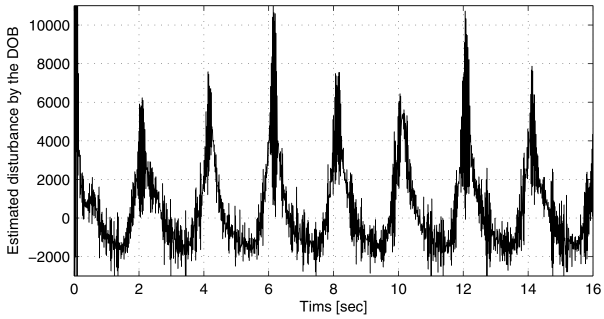


Fig. 11. Estimated disturbance by the DOB.

DOB, the response time was shortened and the closed-loop bandwidth was enlarged significantly. The effectiveness of the DOB was more noteworthy as the locomotion speed increased, which validates that the PD controller with the DOB achieves the desired tracking performance at the entire speed range.

### *4.2 Ground Contact Detection*

Snapshots of a video of a gait experiment are shown in Fig. 10; the right hand side of the Cheetaroid-I was the front direction. The whole motion is divided into two periods based on the motion of right hind leg: (a)-(c) represent the swing period, and (d)-(f) are the stance period. In the stance period, since the feet contact the ground, the ground reaction forces occur and can be measured by appropriate sensing mechanism. Measurement of the ground reaction force is important in the locomotion control because the gait stability is closely related to the ground reaction force.

In this paper, the ground contact detection is conducted through the estimated disturbance by the DOB. The artificial experimental environment was set for the verification of ground contact detection by the DOB. The sinusoidal reference trajectory was used, and the feet contacted the ground slightly for checking the accuracy of the proposed method. Figure 11 shows the estimated disturbance by the DOB, where the estimated disturbance is periodic, and the peaks occur in the estimated disturbance at the ground contact moments. Therefore, the estimated disturbance can be used as the estimate of the ground reaction force with a proposed filtering law, i.e.,

$$\hat{d}_{GND}(t) = fL(s)\left[max(\hat{d}(t) - d_0, 0)\right] \qquad (10)$$

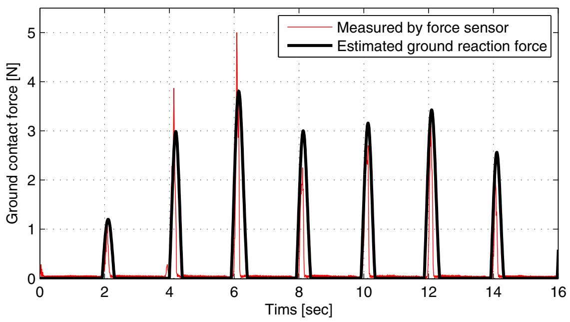


Fig. 12. Ground contact detection.

In (10) $\hat{d}_{GND}$ is the estimated ground reaction force, $f$ is a scaling factor, $L(s)$ is a lowpass filter, $\hat{d}$ is the estimated disturbance by the DOB, and $d_0$ is a threshold value. The estimated disturbance is regarded as the ground contact when it is larger than the threshold value.

Figure 12 shows the ground contact detection results during the sinusoidal tracking experiment, where the estimated ground reaction force and the measured ground reaction force are shown together. The tendency of the estimated ground reaction force was similar to the ground reaction force measured by a force sensor. The error between estimated ground reaction force and force sensor measurement was $0.592N$ in the root-mean-square (RMS). The error was mainly caused by the lowpass filtering, since the high frequency component of ground reaction force was filtered twice by Q-filter and $L(s)$. The estimated ground reaction force preceded the measurement of the force sensor occasionally, and the estimated ground reaction force held longer than the ground reaction force measured by the force sensor as shown in Fig. 12. This is because a force sensing resistor (FSR) sensor was used to measure ground reaction force in the experiment, and the FSR can measure the ground reaction force applied to the sensing area of FSR only (in this case, the diameter of the used FSR was $25mm$). Therefore, the FSR sensor could not measure the ground reaction force even when the feet contacted the ground. On the other hand, the sensing area where the DOB can estimate was not constrained, since the DOB could estimate the total external force that acts on the entire area of the foot. Therefore, wider and faster ground contact detection could be achieved when the ground reaction force is estimated by the proposed DOB-based algorithm.

## 5. CONCLUSIONS

In this paper, the dynamic model of a Cheetaroid-I leg system was analyzed, and the nominal plant model and the range of model variations were obtained through extensive experiments. The parameters of the nominal plant model were further optimized considering the closed-loop stability of the DOB, as well as the closed-loop performance. Also, the ground contact detection was conducted through the magnitude of the estimated disturbance by the DOB. The proposed control system was verified by the experimental results. The tracking performance was remarkably improved by the DOB, and the ground contact detection was available by monitoring the magnitude of the disturbance estimated by the DOB. Consequently, the proposed control system enabled both effective control of a Cheetaroid-I leg system and removal of force sensors for detecting the ground contact. The DOB design was only limited to the distal joint in this paper. The extension of the DOB to the proximal joints is the future work.

## REFERENCES

K. Kong and M. Tomizuka, Design of a Rehabilitation Device Based on a Mechanical Link System. *ASME Journal of Mechanisms and Robotics*, Vol. 4, 035001-1, 2012.

J. Savall, A. Avello, and L. Briones, Two compact robots for remote inspection of hazardous areas in nuclear power plants. *Proc. the IEEE International Conference on Robotics and Automation*, pages 1993-1998, 1999.

K. Nagatani, S. Kiribayashi, Y. Okada, S. Tadokoro, T. Nishimura, T. Yoshida, E. Koyanagi, and Y. Hada, Redesign of rescue mobile robot Quince. *In IEEE International Symposium, Safety, Security, and Rescue Robotics (SSRR),*, pages 13-18, 2011.

K. Kaneko, Towards emergency response humanoid robots, *Mechatronics (MECATRONICS) , 2012 9th France-Japan & 7th Europe-Asia Congress on and Research and Education in Mechatronics (REM), 2012 13th Int'l Workshop*, pages 504-511, 2012.

B. Na, H. Choi, and K. Kong, Design of a Direct-Driven Linear Actuator for Development of a Cheetaroid Robot. *Proc. the IEEE International Conference on Robotics and Automation, Germany*, pages 4008-4013, 2013.

M. Raibert, K. Blankespoor, G. Nelson, R. Playter, and the BigDog Team, BigDog, the Rough-Terrain Quadruped Robot. *Proc. 17th Int Conf. Federation of Automatic Control*, pages 10822-10825, July 2008.

M. A. Lewis, M. R. Bunting, B. Salemi, and H, Hoffmann, Toward Ultra High Speed Locomotors: Design and Test of a Cheetah Robot Hind Limb. *Proc. the IEEE International Conference on Robotics and Automation, Shanghai, China*, pages 1990-1996, 2011.

K. Ohnishi, A new servo method in mechatronics. *Trans. of Japanese Society of Electrical Engineering*, vol. 107-D, pages 83-86, 1987.

K. Fujiyama, M. Tomizuka, and R. Katayama, Digital tracking controller design for CD player using disturbance observer. *Proc. of the Int. Workshop on Advanced Motion Control*, pages 598-603, 1998.

K. Kong, J. Bae, and M. Tomizuka, Control of rotary series elastic actuator for ideal force-mode actuation in human-robot interaction applications. *IEEE/ASME Trans. on Mechatronics*, vol. 14, no. 1, pages 1-14, 2009.

T. Umeno and Y. Hori, Robust speed control of DC servomotors using modern two degrees-offreedom controller design, *IEEE Trans. on Industrial Electronics*, vol. 38, no. 5, pages 363-368, 1991.

S. Oh, and Y. Hori, Disturbance Attenuation Control for Power-Assist Wheelchair Operation on Slopes, *Control Systems Technology, IEEE Transactions on*, vol.PP, no.99, pp.1-1, 2013